Cent. Eur. J. Chem. • 11(4) • 2013 • 485-491
DOI: 10.2478/s11532-012-0182-3

VERSITA

Central European Journal of **Chemistry**

Microstructures and electrode performances of $Mg_{50}Ni_{(50-X)}Pd_x$ alloys

Research Article

Sydney F. Santos[1*], José Fernando R. de Castro[2], Edson Antonio Ticianelli[3]

[1]*CECS, UFABC, 09.210-170 Santo André – SP, Brazil*

[2]*MHNano Ltd., 13566-445 São Carlo, SP, Brazil*

[3]*IQSC, USP, CP 780, 13560-970 São Carlos – SP, Brazil*

Received 2 July 2012; Accepted 15 November 2012

Abstract: Magnesium and several of its alloys can absorb large amounts of hydrogen. This feature is desirable for several technological applications such as solid state hydrogen storage tanks and anodes of nickel-metal hydride (Ni-MH) batteries. For the latter, Mg-Ni alloys are considered very promising due to their high discharge capacities. Conversely, the low stability of Mg-Ni alloys in alkaline electrolytes have hindered their practical use. In the present manuscript, the effects of palladium black addition on the structure and electrochemical properties of the $Mg_{50}Ni_{50}$ (in at.%) alloy were investigated. The studied ternary alloys have general composition of $Mg_{50}Ni_{(50-x)}Pd_x$, with $0 \leq x \leq 5$ (in at.%). These alloys were synthesized by mechanical alloying from pure elements. The alloy powders were characterized by X-ray diffraction (XRD), scanning electron microscopy (SEM), transmission electron microscopy (TEM), and X-ray absorption spectroscopy (XAS) while their electrode performances were evaluated by galvanostatic cycles of charge and discharge. The investigated alloys have multi-phase structures composed of amorphous and nanocrystalline phases, with nano-grain sizes of nearly 5 nm. Concerning the electrode performance, the best results were attained by the $Mg_{50}Ni_{47.5}Pd_{2.5}$ alloy, which kept a high discharge capacity and improved the cycling stability.

Keywords: *Nickel - metal hydride batteries • Hydrogen storage alloys • Mechanical alloying*

© Versita Sp. z o.o.

1. Introduction

Nowadays, the developments in portable electronics, electrical vehicles, and hybrid electrical vehicles are driving the demand for secondary batteries with larger energy densities than those available in market. In the case of nickel-metal hydride (Ni-MH) cells, the increase in energy density is closely related to the increase in electrochemical hydrogen storage capacity of the anode material. Taking the aforesaid into account, Mg-Ni alloys are attracting much attention for anode application due to the high discharge capacity usually displayed by these alloys. Conversely, the low stability of these alloys under galvanostatic cycles of charge and discharge with hydrogen are the main drawback for their practical use [1-4].

Aiming to surpass the above mentioned limitation, several authors have investigated alternatives to improve the electrode performance of Mg-Ni alloys, such as protective coating of alloy particles and addition of alloying elements (*i.e.*, modification of the chemical composition of bulk particle) [1-12]. Until now, the most successful route to improve the electrode performance of these alloys is the addition of alloying elements. Among others, transition metals are the most investigated alloying elements (Ti, Zr, Al, V, Nb, Pt, Pt, *etc.*) for Mg-Ni alloy electrodes [11-18]. Promising results have been reported for the Mg-Ni-Ti system, with limited decrease in the maximum discharge capacity and increase in cycle life performance of the alloy electrodes [17]. Surface analyses of Mg-Ni-Ti alloy electrodes indicate the formation of TiO_2 on top surface of the alloy particles and

* *E-mail: sfsantos91@yahoo.com.br*

decrease in formation of $Mg(OH)_2$. The authors proposed a preferential oxidation of Ti on the surface of the alloys. Moreover, the improvement of the alloy stability over the galvanostatic cycles of charge/discharge was ascribed to the formation of a protective (passive) thin layer of TiO_2 on the surface of the particles, retarding the oxidation / hydroxide formation of magnesium [16,18].

The addition of Pd as catalyst for the (de)hydriding of Mg-Ni alloys was first reported by Zaluski *et al.* [13]. These authors showed that a small amount of Pd (less than 1 wt.%) added to the Mg_2Ni alloy was enough to accelerate the kinetics and decrease the temperature of dehydrogenation. These results were quite interesting; improvements observed in the kinetic properties of hydrides for solid state storage have been ascribed to a spillover mechanism. Investigations of Pd as alloying elements on Mg-Ni alloys are not limited to solid state hydrogen storage applications. Investigations on Mg-Ni-Pd alloy electrodes were carried out by Ma *et al.* [14] and Yamaura *et al.* [15].

Ma *et al.* [8] investigated the electrochemical properties of Mg-Ni-Pd alloys and reported a decay in the degradation rate of the alloy electrodes due to the addition of Pd. Best results were achieved by $(MgNi)_{90}Pd_{10}$ alloy, after 80 h of ball-milling. In the case of Yamaura *et al.* [15] a different processing route was adopted. The investigated Mg-Ni and Mg-Ni-Pd alloys were produced as thin ribbons by a rapidly solidification process known as melt-spinning. The best electrode performances were reported for the $Mg_{67}Ni_{23}Pd_{10}$ (in at.%) alloy which showed improved electrode performance compared to the binary counterpart.

In the present m\anuscript, the Mg-Ni-Pd is revisited. New compositions of this system were synthesized by high-energy ball-milling. In our investigation, partial substitution of Pd for Ni was realized, resulting in the $Mg_{50}Ni_{(50-X)}Pd_X$ alloy series, with $0 \leq x \leq 5$. The amount of Pd in these alloys was limited to low concentrations in other to keep the cost of raw material low. The electrode performances of the investigated alloys are discussed based on the results of structural characterization performed by X-ray diffraction, transmission electron microscopy, scanning electron microscopy, and X-ray absorption near edge spectroscopy. The main targets of this investigation were to obtain Mg-Ni-Pd alloys with enhanced electrode performances, to optimize the amount of Pd in the alloy in order to reduce the cost of raw material and clarify the effect of Pd on the electrode performance of the alloys.

2. Experimental procedure

The general composition of the ternary alloys investigated was $Mg_{50}Ni_{(50-x)}Pd_x$, with x = 0, 1.25, 2.5 and 5 at.% of Pd. These alloys were processed by mechanical alloying using a SPEX 8000 mixer mill. The raw materials for milling were elemental powders of Mg (98% of purity), Ni (99.87% of purity), and Pd black (99.9% of purity). The millings were performed in argon-filled stainless steel vial. The processing parameters adopted for all millings were: (a) ball to powder weight ratio of 10:1; (b) 3 steel balls (1 with 12 mm and 2 with 10 mm of diameter); and (c) 6 h of milling. The as-milled samples were handled in a glove-box under argon to minimize the oxidation. The milling time was selected from previous tests. The Mg-Ni alloy was milled for different times and the obtained powders were cycled galvanostatically. A large discharge capacity was obtained for 6 h of milling. Thus, this milling time was adopted for all the alloys.

The in-situ X-ray absorption spectroscopy (XAS) measurements were conducted at the XAS beam line at the National Synchrotron Light Source (LNLS), Brazil. The radiation was monochromatized using a Si (111) single crystal. The data acquisition set-up comprised of three ionization chambers (incident I_0, transmittance I_t and reference I_R detectors). The reference channel was primarily used for internal calibration of edge position, using pure Ni foils. The measurements were carried out in the transmission mode at the Ni K-edge. The XAS samples were discs, with 2 cm^2 of area, prepared by pressing a mixture of 30 mg of the alloy powder with 40 mg of teflonized carbon (30 wt.%). The XAS data were analyzed using the WinXAS package. Before the XAS measurements, the electrodes were charged with hydrogen with a cathodic current of 5 mA. During the in-situ XAS measurements, a cathodic current of 0.5 mA was maintained.

The investigated alloys have their crystal structures characterized by X-ray powder diffraction (XRD) using a Siemens D5005 diffractometer (Cu - Kα radiation). The microstructures of these alloys were analysed by scanning electron microscopy (SEM) and transmission electron microscopy (TEM), through a Philips XL 30 - FEG and a Philips CM120 microscopes, respectively.

Samples for the electrochemical tests were prepared by cold pressing a mixture of 100 mg of the alloy powder with 100 mg of a blend of carbon black (Vulcan XC-72R) with 33 wt.% of polytetrafluoroethylene (PTFE) binder in a Ni screen with an area of 2 cm^2. The electrochemical measurements were carried out in a three-electrode cell, with a Pt counter electrodes, an Hg/HgO reference

Table 1. Performance of the alloy electrodes.

Alloys	C_{max} (mA h g^{-1})	C_3 / C_{max}	C_6 / C_{max}	C_9 / C_{max}
$Mg_{50}Ni_{50}$	404	0.678	0.460	0.381
$Mg_{50}Ni_{48.75}Pd_{1.25}$	351	0.686	0.478	0.390
$Mg_{50}Ni_{47.5}Pd_{2.5}$	356	0.775	0.643	0.561
$Mg_{50}Ni_{45}Pd_{5}$	258	0.740	0.655	0.596

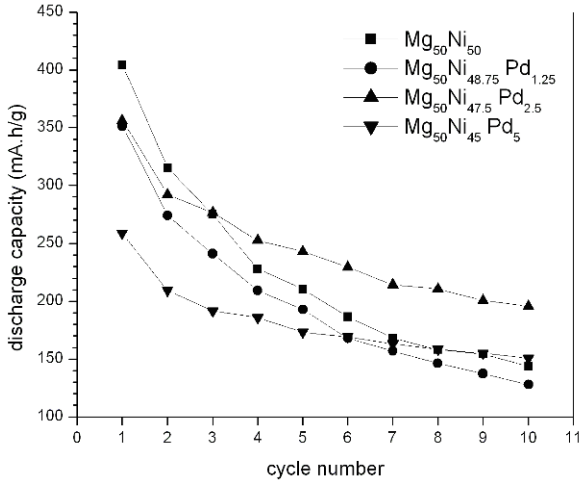

Figure 1. Discharge capacity *versus* cycling number for $Mg_{50}Ni_{(50-x)}Pd_x$ alloy electrodes.

electrode, and a 6 mol L^{-1} KOH electrolyte. The charging current density of the electrodes was 200 mA g^{-1} of active material and the charging current density was 20 mA g^{-1}. The cut-off potential for the discharge steps was –0.4 V (*vs.* Hg/Hg 6 mol L^{-1}).

3. Results and discussion

3.1. Electrode performance

The electrode performance of the alloys was investigated through galvanostatic cycles of charge / discharge which are shown in Fig. 1. From this graph it can be observed that all the investigated alloys showed their maximum discharge capacities in the first cycle, indicating the activated state of these alloys. The $Mg_{50}Ni_{50}$ alloy yielded the highest discharge capacity among the investigated alloys, reaching nearly 400 mA h g^{-1}. This initial high discharge capacity quickly decays after few cycles of charge/discharge. The addition of Pd decreased the maximum discharge capacity of the alloy electrodes to some extent. For x = 1.25 and 2.5 at.% of Pd, the maximum discharge capacity of these electrodes was close to 350 mA h g^{-1}. Further addition of Pd (to 5 at.%) promoted a more pronounced decrease of the maximum discharge capacity. Conversely, the addition of Pd softens the decay of the curve of discharge capacity *vs.* cycling.

In Table 1, the parameters of electrode performances (maximum discharge capacity and retained discharge capacity) are summarized. Taking into account both the maximum discharge capacity and cycling stability the best electrode performance was obtained for the $Mg_{50}Ni_{47.5}Pd_{2.5}$ alloy.

The results obtained for the $Mg_{50}Ni_{47.5}Pd_{2.5}$ alloy can be considering promising due to improved electrode performances obtained for low addition of Pd compared to the results in [14,15].

The formation of $Mg(OH)_2$ on the surfaces of the alloy particles has been ascribed as the main cause of the poor stability of Mg-Ni alloy electrodes over electrochemical cycles of charge and discharge [14]. This Mg hydroxide coating is harmful to the electron-transfer reaction rate and decreases the overall hydrogen absorption rate [16]. This problem has been partially overcame by the addition of transition metals as alloying elements, like Ti, Pd, Pt, *etc.* [2,4-5,7-10, 17-20]. Han *et al.* [18] observed the formation of a thin layer of TiO_2 on the surface of the Mg-Ni-Ti alloy particles. They stated that this oxide layer should be responsible by improving the cycling performance of the electrodes. A similar protection mechanism was proposed for the addition of Zr in Mg-Ni alloys [20]. In both cases, the oxide films may retard the formation of the $Mg(OH)_2$ phase, thus improving the lifetime of the electrode. In the case of Ti and Zr, these elements have almost no mutual solubility with Mg. Moreover, there are no intermediate phases formed in the Zr-Mg and Ti-Mg systems. In some systems, the formation of solid solutions or intermediate phases between the alloying elements and Mg might increase the corrosion resistance of the alloy electrodes. In the case of Mg – Pd, there is almost no solubility of Pd in Mg. On the other hand, the Pd – Ni system shows complete solubility between these elements (isomorphous diagram) [21]. Therefore, in the present case, Pd (noble metal) could act reinforcing the cathodic nature of the alloy electrodes. Nakagawa *et al.* [22] reported that Ti-Pd and Ti-Pt alloys with small amount of noble metals (0.2% of Pd and 0.5% of Pt) had significant improve on their corrosion

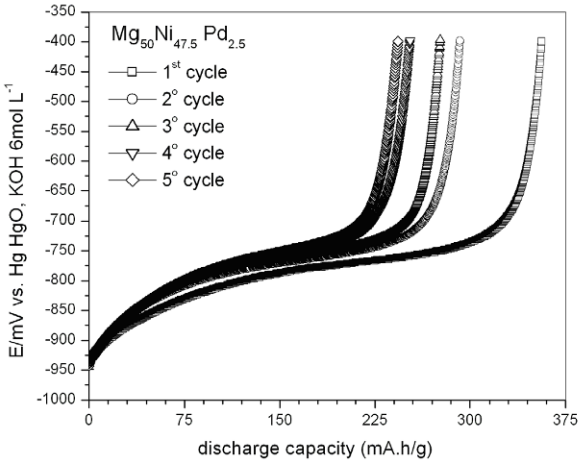

Figure 2. Curves of discharge capacity versus potential of the $Mg_{50}Ni_{47.5}Pd_{2.5}$ alloy for the first 5 cycles.

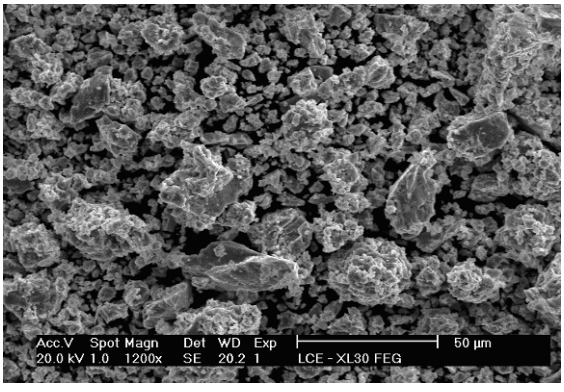

Figure 3. SEM image of the $Mg_{50}Ni_{47.5}Pd_{2.5}$ alloy.

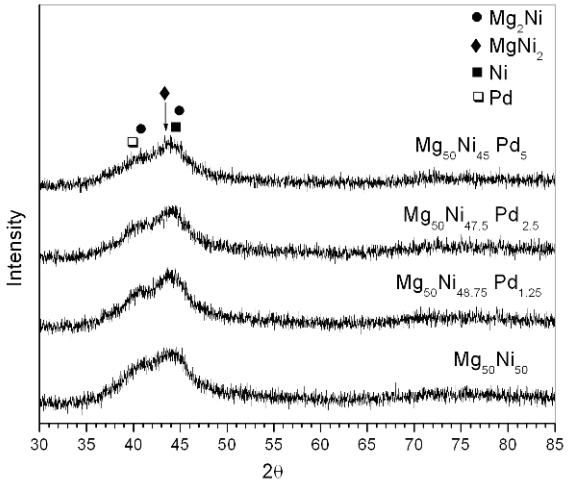

Figure 4. XRD patterns of the $Mg_{50}Ni_{(50-x)}Pd_x$ alloys.

resistances when compared to unalloyed Ti. A similar effect of Pd can be expected for the investigated Mg alloys.

Fig. 2 shows the potential *vs*. discharge capacity curves for the first five cycles of the $Mg_{50}Ni_{47.5}Pd_{2.5}$ alloy. It can be observed that the discharge plateaus are sloping, indicating heterogeneities in the alloy which could have chemical or structural natures [2]. In fully amorphous alloys, the absence of plateau of potential (or plateau of pressure, in gas phase hydriding) is expected due to the broad spectrum of potential energy of the sites available for hydrogen occupation, even if a crystalline alloy of the same chemical composition exhibits a plateau of potential (or plateau of pressure). This behavior was first reported by Maeland and Libowitz [23], which studied the hydrogenation of amorphous and crystalline ZrNi alloys. These authors observed a very flat plateau of pressure during the hydrogenation of the crystalline ZrNi compound, typical of the formation of a metal hydride. When these authors performed the hydrogenation of the amorphous alloy with the same chemical composition, they observed the absence of a plateau of pressure. Smilar behavior were reported by different authors [24,25]. In the case of the current investigation, the alloy electrodes are not fully amorphous and the sloping plateaus observed can be regarded as a combination of the hydrogenation of amorphous and crystalline phases. Further inference on the microstructure of the alloys is performed in the following section.

3.2. Microstructural characterization

After milling, the obtained powders were characterized by scanning electron microscopy (SEM) using secondary electrons (SE) detector. A similar morphology of the powders was observed in all the investigated alloys. This feature is due to the similar chemical composition of the alloys and the adoption of the same processing parameters for all the alloys. A typical SEM image of a milled sample is shown in Fig. 3. In this image, it is possible to observe a wide variation in particle sizes, although in general the powder is mainly composed of large agglomerates of fine particles and some large and coarse particles. This heterogeneity in particles size is probably related to the relatively short time of milling adopted to synthesize the alloys (6 h).

The X-ray diffraction (XRD) patterns of the $Mg_{50}Ni_{(50-x)}Pd_x$ alloys are shown in Fig. 4. In all XRD patterns a broad band can be observed ranging from nearly 35 to 50º, indicating the predominance of an amorphous structure. In addition to this band, small broadened diffraction peaks can also be detected. These features indicate that the alloys have microstructures composed of nanocrystalline phase(s) dispersed on an amorphous matrix. These nanocrystalline phases were identified as: Mg_2Ni, $MgNi_2$, Ni and Pd, as indicated by the XRD patterns.

Transmission electron microscopy (TEM) results for the $Mg_{50}Ni_{47.5}Pd_{2.5}$ alloy are shown in Figs. 5a-5c.

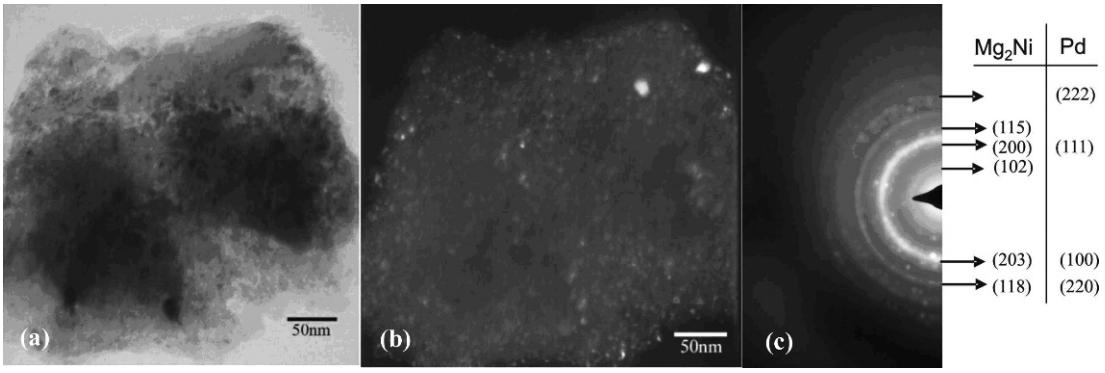

Figure 5. TEM bright field image (a), dark field image (b), and the corresponding SAEDP (c) of the $Mg_{50}Ni_{47.5}Pd_{2.5}$ alloy.

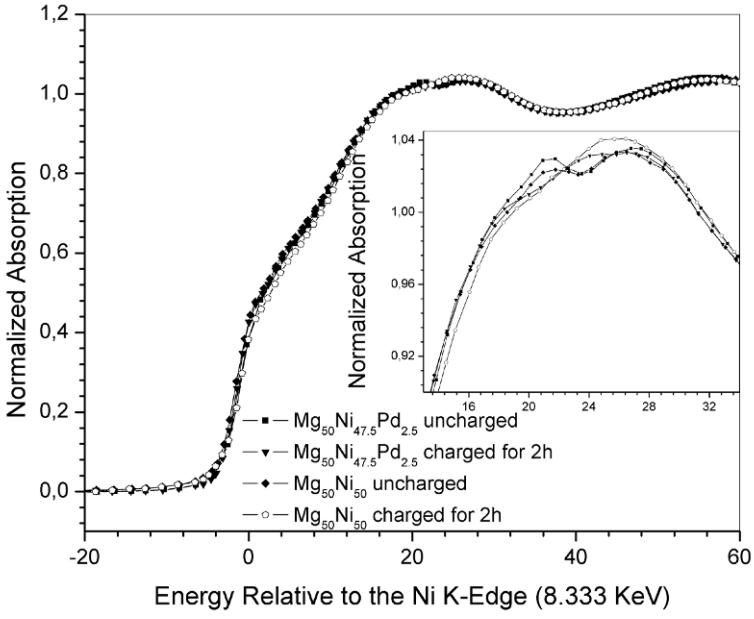

Figure 6. XANES spectra at the Ni K-edge for charged and uncharged $Mg_{50}Ni_{50}$ and $Mg_{50}Ni_{47.5}Pd_{2.5}$ alloys.

An alloy particle can be observed in bright-field image (Fig. 5a). The nanostructured nature of this particle and the average crystallite size of about 5 nm can be estimated from dark-field image (Fig. 5b). Indexing the selected area electron diffraction patterns (SAEDPs), the respective phases were identified: tetragonal Mg_2Ni (JCPDS 35-1225) and face centered cubic Pd (JCPDS 46-1043) (Fig 5c). No diffraction patterns from Mg-Pd phases were identified. The partial replacement of Pd for Ni in Mg-Ni phases can not be completely disregarded because the Ni-Pd alloy system exhibits an isomorphous phase diagram [21]. Moreover, the incorporation of Pd into the amorphous phase can also occur.

3.3. X-ray absorption spectroscopy

In Fig. 6 XANES spectra at Ni-K edge of $Mg_{50}Ni_{50}$ and $Mg_{50}Ni_{47.5}Pd_{2.5}$ alloys in uncharged and 2 h charged conditions are shown. Small oxidation of Ni in uncharged alloys (as-milled) is indicated by the increased intensity of the pre-edge hump peaks (around 18–25 eV). The decrease of the edge humps after 2 h of charging indicated reduction of Ni oxide in the alloys. The similarlity between results on Ni K-edge absorption between $Mg_{50}Ni_{50}$ and $Mg_{50}Ni_{47.5}Pd_{2.5}$ alloys indicated that the increase in the alloy stability is not related to Ni oxidation, inferring that Pd addition probably affected the oxidation of Mg in the alloys.

3.4. Discussion

Combination of XRD, XANES and TEM results clearly indicate the alloys have structures composed of an amorphous phase with nanocrystalline particles dispersed in its microstructure. The predominance of a disordered structure in the investigated alloys

is in agreement to the sloping plateaus observed during discharging of the electrodes (Fig. 2). This feature is related to the partial amorphous structure of the alloy and, consequently, the sites available for hydrogen occupation have a broadened distribution of potential energies [24]. The amorphous structure in Mg-Ni electrode alloys is quite desirable. Liu *et al.* [25] investigated the Mg_xNi_{100-x} alloy series, with x ranging from 10 to 90 wt.%. These authors reported that fully amorphous alloy was obtained between 30 to 70 wt.% of Mg and yielded the best electrode performances.

As previously mentioned the formation of $Mg(OH)_2$ on the surface of the particles plays a major role on the degradation of the electrode performance of Mg-Ni alloys. The positive effect of Pd on the stability of the alloys was experimentally observed, even for low Pd concentration. Similar behavior has been previously reported in literature for Mg-Ni alloys and Ti alloys [14,15,22]. Until now, there is a lack of information regarding the mechanism of action of Pd that prevents the oxidation of such alloys; however, some considerations can be introduced: i) first, Pd can increase the cathodic behavior of Mg-Ni alloys preventing / retarding their oxidation. There was not observed during the formation of intermediate Mg-Pd phases, and the interaction of Pd with the alloy could take place by partial replacement of Pd for Ni, since these elements form an isomorphous diagram (have complete mutual solubility) as discussed in section 3.1; ii) The decay in discharge capacity of Mg-Ni alloy electrodes has been ascribed to the formation of $Mg(OH)_2$ on the particles hindering the electron transfer reaction therefore decreasing the amount of active material for hydrogen storage in the alloy. Thus, it is probable that Pd can retard the formation of this hydroxide phase, in spite of the mechanism involved in this reaction being unclear yet; iii) The results of XANES indirectly indicate that Pd addition affected the corrosion resistance of Mg, since no changes were observed for Ni absorption band and Pd is more stable than Ni in alkaline electrolyte.

4. Conclusions

The utilization of Pd as alloying element of $Mg_{50}Ni_{50}$ alloy is very effective to increase the stability of the alloy electrodes. The amount of Pd in the alloy must be limited to low concentration in order to avoid an excessive drop in the maximum discharge capacity. Moreover, the utilization of low amounts of Pd in the alloy electrodes is mandatory due to the cost of this raw material. Thus, considering all the aforementioned constrains the best performance was yielded by the $Mg_{50}Ni_{47.5}Pd_{2.5}$ alloy.

Concerning the microstructure of the investigated alloys, these are composed of amorphous and nanostructured Mg_2Ni, $MgNi_2$, and Ni phases, with the possibility of the Pd phase in the alloys containing the metal.

Further investigations are still necessary to fully understand the mechanism by which Pd promotes improvement of the cyclic stability of the alloy electrodes. But based on our results it is possible to infer that Pd acts by reinforcing the cathodic behavior of the alloys and improving the corrosion behavior of Mg.

Acknowledgements

The authors wish to thanks the Brazilian institutions FAPESP and CNPq for financial support. We are also in debt with the National Synchrotron Light Source (LNLS) in Campinas – SP, Brazil, by the beamline time for XANES experiments.

References

[1] M.A. Fetcenko, S.R. Ovshinsky, B. Reichman, K. Young, C. Fierro, A. Zallen, W. Mays, T. Ouchi, J. Power Sources 165, 544 (2007)
[2] S.F. Santos, T.T. Ishikawa, E.A. Ticianelli, In: J.R. Telle, N.A. Pearstine (Eds.), Amorphous Materials: Research, Technology and Applications (Nova Science, New York, 2009) 219
[3] P.H.L. Notten, M. Ouwerkerk, H. van Hal, D. Beelen, W. Keur, J. Zhuo, H. Feil, J. Power Sources 129, 45 (2004)
[4] X. Zhao, L. Ma, Int. J. Hydrogen Energy 34, 4788 (2009)
[5] S.F. Santos, J.F.R. de Castro, T.T. Ishikawa, E.A. Ticianelli, J. Alloys Compd. 434, 756 (2007)
[6] S.F. Santos, J.F.R. de Castro, T.T. Ishikawa, E.A. Ticianelli, J. Mater. Sci. 43, 2889 (2008)
[7] C. Rongeat, L. Roué, J. Alloys Compd, 404, 679 (2005)
[8] E.C. Souza, J.F.R. de Castro, E.A. Ticianelli, J. Power Sources 160, 1425 (2006)
[9] L.-J. Huang, Y.-X. Wang, J.-G. Tang, J.-Q. Liu, Y. Wang, J.-X. Liu, Z. Huang, Int. J. Electrochem. Sci. 6, 6200 (2011)
[10] J.-J. Jiang, M. Gasik. J. Power Sources 89, 117 (2000)
[11] E. Souza, E.A. Ticianelli, Int. J. Hydrogen Energy

32, 4917 (2007)
[12] J.F.R. de Castro, S.F. Santos, F.R. Nikkuni, T.T. Ishikawa, E.A.Ticianelli, J. Alloys Compd. 498, 57 (2010)
[13] L. Zaluski, A. Zaluska, P. Tessier, J.O. Ström-Olsen, R. Schulz, Mater. Sci. Forum 225, 853 (1996)
[14] T. Ma, Y. Hatano, T. Abe, K. Watanabe, J. Alloys Compd. 372, 251 (2004)
[15] S.-I. Yamaura, H.-Y. Kim, H. Kimura, A. Inoue, Y. Arata, J. Alloys Compd. 347, 239 (2002)
[16] C. Rongeat, M.H. Grosjean, S. Ruggeri, M. Dehmas, S. Bourlot, S. Marcotte, L. Roué, J. Power Sources 158, 747 (2006)
[17] Y. Hatano, T. Tachikawa, D. Mu, T. Abe, K. Watanabe, S. Morozumi, J. Alloys Compd. 330, 816 (2002)
[18] S.-C. Han, P.S. Lee, J.-Y. Lee, A. Zuttel, L. Schlapbach, J Alloys Compd 306, 219 (2000)
[19] H. Ye, Y.Q. Lei, L.S. Chen, H. Zhang, J. Alloys Compd. 311, 194 (2000)
[20] H. Y. Lee, N. H. Goo, W. T. Jeong, K. S. Lee, J. Alloys Compd. 313, 258 (2000)
[21] T.B. Massalski, ASM/NIST Data Program for Alloy Phase Diagrams on CD-ROM, OH 44073, USA.
[22] M. Nakagawa, S. Matsuya, K. Udoh, Dental Mater. J. 21, 83 (2002)
[23] A.J. Maeland, G.G. Libowitz, J. Less-Commomn Metals 101, 131 (1984)
[24] R. Kirchheim, F. Sommer, G. Schluckebier, Acta Metall. 30, 1059 (1982)
[25] W. Liu, H. Wu, Y. Lei, Q. Wang, J. Wu, J. Alloys Compd. 252, 234 (1997)